Soil & Tillage Research 205 (2021) 104763

Contents lists available at ScienceDirect

Soil & Tillage Research

journal homepage: www.elsevier.com/locate/still

Spatiotemporal variations in soil organic carbon and their drivers in southeastern China during 1981-2011

Enze Xie[b,c], Yanxia Zhang[a,d,*], Biao Huang[a,c,*], Yongcun Zhao[b,c], Xuezheng Shi[b,c], Wenyou Hu[a,c], Mingkai Qu[a,c]

[a] Key Laboratory of Soil Environment and Pollution Remediation, Institute of Soil Science, Chinese Academy of Sciences, Nanjing, 210008, China
[b] State Key Laboratory of Soil and Sustainable Agriculture, Institute of Soil Science, Chinese Academy of Sciences, Nanjing, 210008, China
[c] University of Chinese Academy of Sciences, Beijing 100049, China
[d] School of the Environment, Nanjing Normal University, Nanjing 210023, China

ARTICLE INFO

Keywords:
Soil organic carbon
Drivers of SOC
Land use change
Carbon inputs
Geographical detector model

ABSTRACT

Understanding the spatiotemporal distribution of soil organic carbon (SOC) and its controlling factors is extremely important for improving soil quality and developing sustainable management practices. We quantified spatiotemporal variations in SOC in three typical regions (Shuyang, Rugao, and Shanghai) in southeastern China during 1981–2011, by using geographically weighted regression (GWR), and explored the drivers with a geographical detector method. A total of 219 topsoil samples were collected in the three regions to measure the SOC in 2011, and a total of 109 SOC data for 1981 were obtained from the soil survey reports of Shuyang, Rugao, and Shanghai, which involved in the database of the second national soil survey of China. The results showed that the mean SOC contents in 2011 were 14.68 g kg^{-1}, 9.55 g kg^{-1}, and 18.00 g kg^{-1} in Shuyang, Rugao, and Shanghai, respectively. The topography (q = 0.60) and the sand content of the soil (q = 0.70) were the main drivers of the spatial variability in the SOC in Shuyang and Rugao, while the carbon inputs (q = 0.68) predominantly explained the spatial heterogeneity of the SOC in Shanghai. Significant increases in SOC storage occurred in Shuyang and Rugao from 1981 to 2011, with increase rates of 0.55 t ha^{-1} yr^{-1} and 0.26 t ha^{-1} yr^{-1}, respectively. Land use change (dryland farming to rice cultivation) was identified as the largest driver of the SOC increases in Shuyang and Rugao (q values of 0.16 and 0.09, respectively), followed by increasing carbon inputs (0.14 and 0.07). However, the SOC storage in Shanghai rapidly decreased at a rate of −0.38 t ha^{-1} yr^{-1} during 1981–2011. The land use change from wetlands to rice cultivation was the primary reason for the decreasing SOC (q = 0.24), and a net decrease in carbon inputs between 1981 and 2011 was another main driver of the reduction in the SOC in Shanghai (q = 0.14). Our results from this study provide important information on the spatiotemporal changes in SOC and its drivers to the scientific community and decision-makers, for the development of management strategies to sustain soil fertility in many areas with rapid economic development and increasing populations.

1. Introduction

Soil organic carbon (SOC) is commonly considered as a basic indicator of soil fertility (kononova, 1966; Ondrasek et al., 2019; Tiessen et al., 1994), which not only affects crop production (Fernandes et al., 2019; Liu et al., 2011; Wood et al., 2018) and soil functions (Jensen et al., 2019), but also plays a critical role in maintaining sustainable development of terrestrial ecosystems (Lehmann and Kleber, 2015; Liu et al., 2017b). The accumulation or loss of SOC mainly depends on inherent factors such as the soil physical and chemical properties, and external environmental factors that directly or indirectly affect the balance between the organic inputs (e.g., straw/residue return) and outputs (e.g., soil microbial decomposition) (Frouz, 2018; Fujisaki et al., 2018; Hancock et al., 2019). Thus, understanding the spatiotemporal distribution of changes in SOC and its drivers is extremely essential for guiding the management of soil nutrients, assessment of soil quality, and formation of agricultural policy.

Numerous methods have been used to estimate the spatiotemporal distribution of changes in SOC based on the relationships between SOC and its associated drivers. Geographically weighted regression (GWR), which was developed by Brunsdon et al. (1996) and Fotheringham et al. (2002), is one of the widely-used methods because it provides the

* Corresponding authors.
E-mail addresses: yxzhang@issas.ac.cn (Y. Zhang), bhuang@issas.ac.cn (B. Huang).

https://doi.org/10.1016/j.still.2020.104763
Received 24 February 2020; Received in revised form 15 June 2020; Accepted 1 July 2020

advantage of varying local estimations of regression coefficients at different spatial locations. For example, Costa et al. (2018) compared and evaluated the accuracy of multiple linear regression (MLR) and geographically weighted regression (GWR) models to predict SOC, and demonstrated that the GWR model showed a better performance for the prediction of the SOC in the southeast of Brazil. Moreover, through the use of a mixed GWR model (MGWR), Zeng et al. (2016) revealed the spatial distribution patterns and the accuracy of SOC predictions in two typical study areas of China. They found that the errors produced by MGWR were lowest when compared with other methods such as ordinary kriging and multiple linear regression, indicating that MGWR was highly competitive for SOC prediction. However, with differences in these studies focusing on predictive approaches, multiple factors that affect spatiotemporal changes in SOC have drawn increased amounts of attention in recent years, including natural factors such as soil texture, topography, and vegetation (Singh et al., 2019; Takata et al., 2007; Zheng et al., 2019), and anthropogenic factors such as framing practices (e.g., tillage, fertilizer, and straw/residue return) (Magdoff and Weil, 2004; Zhao et al., 2018).

In general, environmental factors are widely applied to describe the spatial variability in SOC. For example, soil texture, particularly for clay content, plays a significant role in protecting SOC by promoting the stability of soil aggregation (Johannes et al., 2017). Topographic features such as altitude and slope control the redistribution of hydrothermal conditions, thereby indirectly affecting the rate of SOC decomposition (Fissore et al., 2017; Zhu et al., 2019a). Vegetation also affects SOC because of the increased organic carbon inputs from plant straw/residue and the exchange of carbon with the atmosphere (Wang et al., 2019). However, human disturbance can directly affect temporal changes in SOC by controlling the balance of inputs (straw/residue inputs; manures and organic fertilizers) (Ogle et al., 2005; Wang et al., 2015), and outputs such as tillage, which accelerates the rate of SOC decomposition by breaking the soil aggregates (Jat et al., 2019). In addition, the land use change induced by the process of rapid urbanization is an important anthropogenic factor affecting spatial or spatiotemporal changes in SOC. For example, Vasenev et al. (2014) reported that the spatial distribution of soil organic carbon was closely related to the continuing urban sprawl in Moscow, Russia, and explained more than 30% of the total variability. Similarly, Song et al. (2019) also found that land use change has been an important driver of soil organic carbon (SOC) change in the Yangtze River Delta in China, where the urban areas exhibited higher SOC contents than the croplands due to the input of green manure in urban-rural ecotones and high carbon sequestration in urbanized lands (e.g., urban parks).

SOC has been widely investigated in the Jiangsu-Shanghai region of China which has been experiencing intensive cultivation, significant industrialization and rapid urban expansion since the 1980s (Fei et al., 2019; Lu et al., 2017; Pan et al., 2009; Zhang et al., 2019a). However, studies related to the spatial or spatiotemporal changes in SOC and its drivers are still under-researched in areas with rapid economic growth in China. To consider the effect of economic growth on the spatiotemporal changes of SOC, we selected three typical cities (Shuyang, Rugao, and Shanghai) that represented different levels of economic development across the Jiangsu-Shanghai region. Specifically, soil types among the three selected cities significantly differed (Fig. 1), the Anthrosols was the main type in Shanghai, which had higher SOC (Yang, 2017), while the Cambosols and Anthrosols were the main types in Shuyang and Rugao, respectively, both of which had lower SOC (Huang et al., 2017).

The objectives in this paper are to 1) predict the spatiotemporal changes in the SOC in Shuyang, Rugao, and Shanghai during the period of 1981–2011; 2) identify the possible factors affecting the spatial distribution of SOC; 3) explore the potential factors dominating the temporal changes in the SOC and in Shuyang, Rugao, and Shanghai.

2. Materials and methods

In this study, the basic framework for illustrating all steps of the data analysis is shown in Fig. 2. First, the legacy SOC data (obtained from the second National Soil Survey of China) and measurements of SOC were used to delineate the spatial maps in 1981 and 2011, respectively, and then the spatial patterns of the changes in SOC were generated by subtracting the spatially-distributed SOC maps between 1981 and 2011. Finally, we analyzed the drivers controlling spatiotemporal changes of SOC through a geographical detector model.

2.1. Study area

Soil samples were collected from two county-level cities in Jiangsu Province (Shuyang and Rugao), and two typical districts in Shanghai (Songjiang and Qingpu districts) (Fig. 1). Shuyang County is located between the latitudes of 118°30′ E to 119°10′ E and the longitudes of 33°53′ N to 34°25′ N, covering 2298 km^2 of land area. With a warm temperate monsoon climate, the area has an average annual temperature of 14.1 °C and an annual rainfall of 918 mm (from 552 to 1480 mm). The gentle topography of the study area is characterized by low elevations in most areas (fewer than 7 m above sea level), while the areas with the highest elevation (approximately 43 m) were mainly distributed in southwestern parts of the study area. Rugao covers approximately 1600 km^2 between the longitudes of 32°00′ N to 32°30′ N and the latitudes of 120°20′ E to 120°50′ E. Rugao has a subtropical monsoon climate, with an average temperature of 14.6 °C and a mean rainfall of 1060 mm (Huang et al., 2007). The elevations in the study area varies from −13 to 30 m above sea level. Songjiang and Qingpu located in western Shanghai also have a subtropical monsoon climate with an annual average temperature of 17.6 °C and a mean precipitation of 1173 mm (Fei et al., 2019). The altitude is between −48 m and 90 m. According to the Shanghai Statistical Yearbook, the total coverage of Songjiang and Qingpu districts is 1275 km^2 (Shanghai Bureau of Statistics, 2010).

Soil samples in 1981 were compiled from typical soil profiles in each county's soil monograph, which were part of the second national soil survey in China. The second national soil survey was carried out during 1979–1994, covering over 2400 counties in China (Shi et al., 2004). This nationwide survey provides the most comprehensive soil data information that are widely applied for soil quality monitoring, agricultural management, and ecosystems health assessment in China (Guo et al., 2010; Yan et al., 2011; Zhao et al., 2018). Specifically, the sample sites were selected by the rule that covered typical soil types and topographic characteristics in each county. Soil samples were collected to various depths and then were analyzed in laboratory to obtain data on soil physicochemical properties such as soil texture, soil organic matter (SOM), bulk density (BD). In addition, related background information (e.g., text descriptions of sampling locations, soil types, vegetation types, topography, and land use) was also recorded in detail. In general, tens or hundreds of observations arrayed by soil type were reported in soil monograph of each county (Han et al., 2018). In the study area, the topsoil data (0–20 cm) on SOM and BD were used to map spatial distributions of SOC in 1981.

2.2. Soil sampling and analysis

A total of 109 topsoil data respectively on soil organic matter (SOM) and bulk density (BD) in 1981 were obtained from the soil survey reports of the three counties (39 in Shuyang (Soil Survey Committee of Shuyang County, 1984), 49 in Rugao (Soil Survey Office of Rugao County, 1987), and 21 in Shanghai (Soil Survey Office of Shanghai City, 1988)) **(Figure S1)**. The text descriptions of the soil types and sampling locations were also collected from these soil monographs. So far, these materials are still the most detailed legacy data that are available for extracting historical information on the soil properties of the study

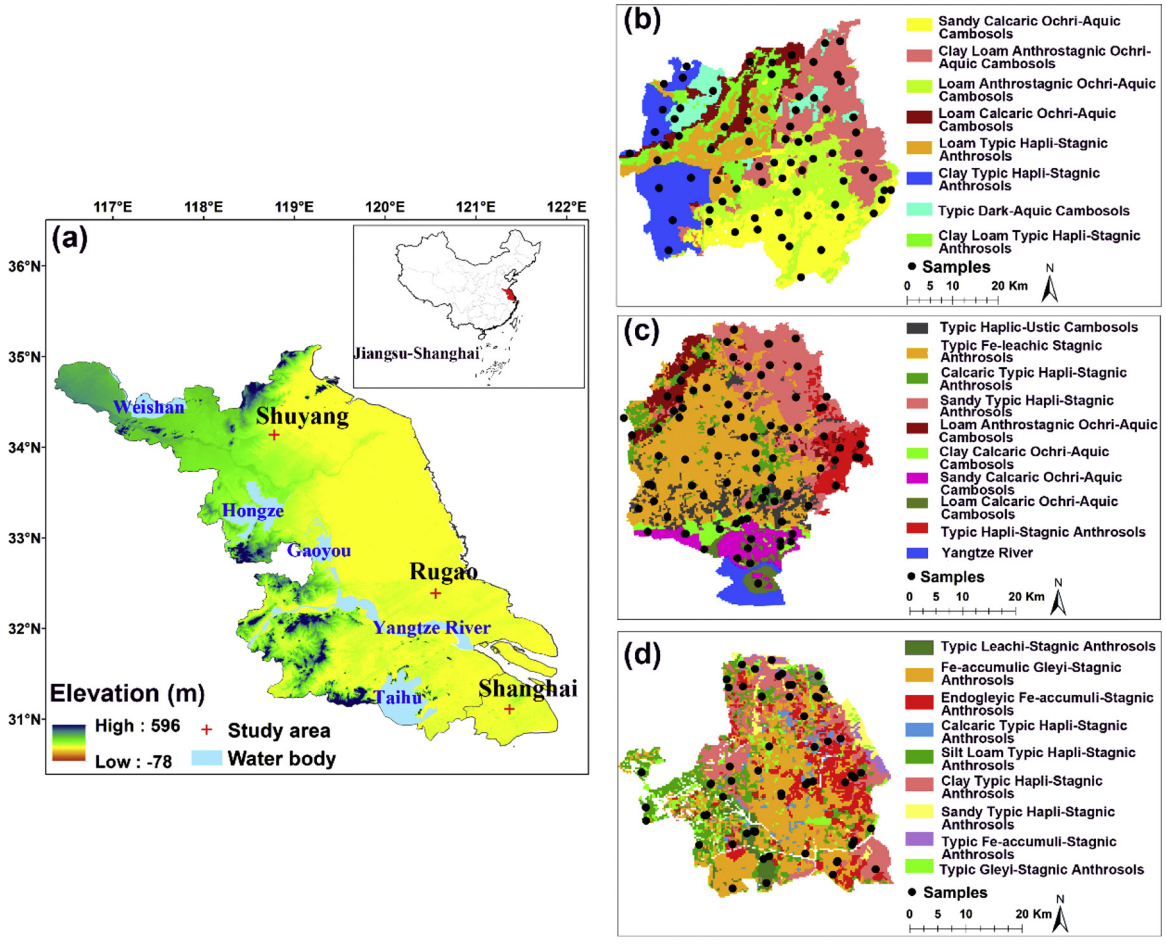

Fig. 1. Geographic location with a relative elevation map of the study area (a). The soil types and soil sampling distributions respectively in Shuyang (b), Rugao (c), and Shanghai (d) in 2011.

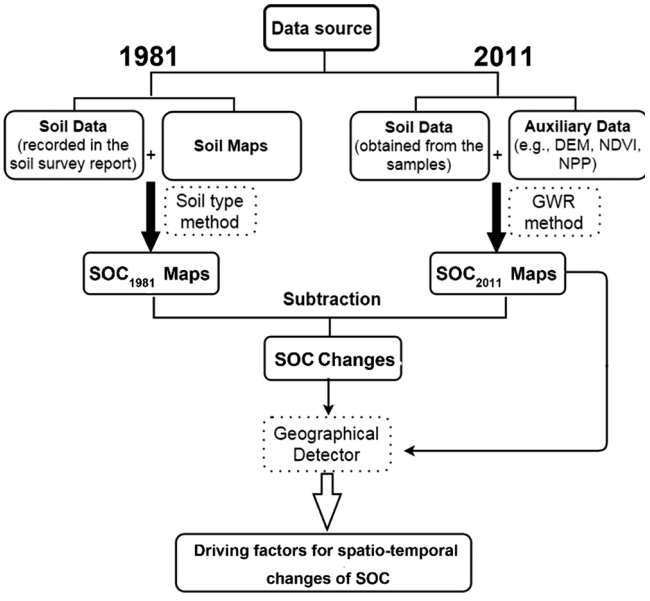

Fig. 2. A framework for the data analysis in this research.

area.

A total of 219 topsoil samples were collected in 2011 for a relatively thorough coverage of the study areas (72 in Shuyang, 88 in Rugao, and 59 in Shanghai). These sample sites almost covered all sample locations in 1981, and we added more samples based on different soil types, topography and land uses **(Figure S1)**. All sample locations were recorded by a hand-held GPS. The soil types, topography, and land use types were recorded as well.

The SOM contents were determined using the potassium dichromate oxidation with external heating method, and the BDs were measured using cutting ring method (ISSCAS, 1978). We transferred SOM into SOC by the content of SOM multiplying 0.58 (Zhao et al., 2018). The spatial distributions of BD in 1981 and 2011 were presented in **Figure S2**.

Other soil properties were also determined. The soil pH was determined by using the glass electrode method with a soil: water ratio of 1:2.5 (ISSCAS, 1978). The soil available P (Avp) was extracted with 0.5 mol L^{-1} $NaHCO_3$ and then determined following the molybdenum blue colorimetric method. The available K (Avk) in the soil was extracted with 1 mol L^{-1} NH_4OAc and determined with a flame photometer (Zhao et al., 2008). The soil total phosphorus (TP) and total potassium (TK) were all determined by the method of molybdate colorimetric measurement after digestion with concentrated $HClO_4$-H_2SO_4, and the flame photometry method after melting with sodium hydroxide (Gao et al., 2019; Shen et al., 2019). The soil particle-size distribution was measured with the pipette extraction method (Indorante et al., 1990), and was classified in terms of the percentages of clay content (< 0.002 mm) (denoted as Clay hereafter), silt content ($0.002-0.05$ mm) (denoted as Silt hereafter), and sand content ($0.05-2$ mm) (denoted as Sandy hereafter).

2.3. Spatial analysis of auxiliary variables

Soil properties (BD, pH, Avp, Avk, TP, TK, Clay, Silt, Sandy) were interpolated into raster layers (spatial resolution of 300 m × 300 m), which were considered as auxiliary variables for the prediction of the spatial distribution of SOC. We also considered other environmental variables such as topography (e.g., elevation, slope, and aspect) that derived from digital elevation model (DEM)), vegetable indexes (e.g., normalized difference vegetation index (NDVI)), and net primary production (NPP). The DEM was obtained from RESDC (2018a) with a spatial resolution of 90 m. The 1 km × 1 km annual NDVI (2005 − 2011) was obtained from Xu (2018). The 1 km × 1 km annual NPP (2005 − 2011), which derived from RESDC (2018c), was used to calculate the crop carbon input (C inputs) into agricultural soils using the approach in Zhou et al. (2013) (e.g., estimate carbon input from aboveground and belowground crop straw/residues based on the grain: straw ratio of staple crop in the study area). The environmental variables of elevation, the NDVI, and C input were transformed into raster layers with a resolution of 300 m × 300 m.

In this study, the relationships (Pearson correlation coefficients) between the predicted factors and the SOC were shown in **Table S1**, and the factors significantly related to SOC ($p < 0.05$) were chosen to predict the spatial distribution of SOC. The results indicated that in Shuyang, the factors with p values < 0.05 were BD, Avk, TP, TK, Clay, elevation, NDVI and C input. In Rugao, BD, Avk, Sandy, Silt, Clay, elevation, and NDVI were selected. In Shanghai, the related factors were BD, Silt, Clay, pH, and C input.

2.4. Mapping the spatiotemporal variations in SOC

2.4.1. Geographical weighted regression (GWR) for SOC in 2011

GWR as an extension of the traditional multiple linear regression, has clearly reflected the spatial relationships between dependent and independent variables (Zhang et al., 2011). Therefore, this model was used to predict the spatial variability of SOC in Shuyang, Rugao, and Shanghai in 2011. To understand how useful GWR model, cross-validation method was used to estimate the predictive accuracy of GWR model. The result of model evaluation indicated that the GWR model showed a better performance of SOC prediction in the study area when compared with other methods (e.g., random forest model and regression kriging methods) (**SM1 Model validation**, **Table S2**).

The GWR model takes the spatial locations of samples into consideration and ensures that the regression coefficients are local estimates, thus generally leads to the following equation (Fotheringham et al., 2002):

$$y_j = \beta_0(m_j, n_j) + \sum_{i=1}^{k} \beta_i(m_j, n_j)x_{ij} + \varepsilon_j \quad (1)$$

where (m_j,n_j) is the coordinates of the sample point at jth location, y_j represents the value of the dependent variable at location (m_j,n_j), $\beta_0(m_j,n_j)$ is the regression intercept at the location (m_j,n_j), $\beta_i(m_j,n_j)$ is the regression coefficient at the location (m_j,n_j), k is the total number of independent variables, ε_j is the random error at the jth location, and X_{ij} is the ith independent variable at location (m_j,n_j). Nevertheless, the parameters in the GWR model area are estimated by the following weighting function:

$$\beta\hat{}(m_j, n_j) = [\mathbf{X^T W}(m_j, n_j)\mathbf{X}]^{-1}\mathbf{X^T W}(m_j, n_j)\mathbf{Y} \quad (2)$$

where $W(m_j,n_j)$ is the matrix of spatial weights at the location (m_j,n_j), X is an independent data matrix, X^T is its transpose, and Y is a dependent data vector. The weights were determined by the spatial kernel method. In this research, a typical weighting function (Gaussian function) was used for the SOC prediction (Yang et al., 2019), which can be written as follows:

$$W_{ij} = \exp[-0.5 \times (\frac{d_{ij}}{b})^2] \quad (3)$$

where W_{ij}, a weighting function representing the influence between location i and j, is the Gaussian distance-decay function, d_{ij} represents the Euclidean distance between location i and j, and b represents the kernel bandwidth that describe the extent to which the resulting local calibration results are smoothed (Fotheringham et al., 2002). In this study, the bandwidth is an adaptive number that corresponds to the number of nearest neighborhoods. Therefore, the bandwidth is the key parameter controlling the GWR results (Kang and Dall'erba, 2016; Wang et al., 2020).

2.4.2. A soil type–based method (ST) for SOC in 1981

As the Global Positioning System (GPS) was not available in the early 1980s in China, positions of all sampling sites were recorded by text descriptions in 1981. For example, the village name of a specific point was usually recorded, combined with the direction and distance of this point to the center of the village. Thus, the positions of sampling sites can only be determined imprecisely. The soil type-based (ST) method, which is used to map spatial distributions of SOC in 1981, is to consider the mean SOC value of samples from one specific soil type as the SOC value of this soil type based on the soil map of the study area (Meersmans et al., 2011; Zhao et al., 2014b). Since the ST method is only considered the linkage between the mean SOC contents and soil types, accurate spatial location information is not necessary (Zhao et al., 2006).

2.4.3. Changes in the distribution of SOC over the period of 1981–2011

Based on the spatial distribution of SOC (Shuyang, Rugao, and Shanghai) in 1981 and 2011, the overall changes in the SOC in Shuyang, Rugao, and Shanghai during 1981–2011 were determined by subtracting the predicted SOC maps for 2011 from the predicted SOC maps for 1981.

The spatial predictions of the SOC in Shuyang, Rugao, and Shanghai were carried out using R software (Version 3.6.1), and the GWR method was implemented in the GWmodel package (Brunsdon et al., 1996). Spatial maps of the SOC were generated with ArcGIS 10.2 software.

2.5. Estimation of SOC storage changes

SOC storage in topsoil (0 − 20 cm) was calculated using Eqs. (4)–(6)

$$SOCD = SOC \times BD \times Depth \times (1 - RF)/10 \quad (4)$$

$$SOCS = \sum_{i=1}^{n} A_i \times SOCD_i \quad (5)$$

$$\Delta SOCS = SOCS_{2011} - SOCS_{1981} \quad (6)$$

where *SOCD* is the soil organic carbon density (t ha^{-1}), *SOC* is the soil organic carbon content (g kg^{-1}), *BD* is bulk density (g cm^{-3}), *Depth* is the thickness of the layer (20 cm), and *RF* is the volume fraction of rock fragments (> 2 mm). *SOCS* is the total soil organic carbon storage. *i* is the number of soil grid in the study area ($i = 1, 2, \ldots, n$). A_i is the surface area of each soil grid, and $SOCD_i$ is the soil organic carbon density of each soil grid. $\triangle SOCS$ is the change of soil organic carbon storage in 1981 ($SOCS_{1981}$) and in 2011 ($SOCS_{2011}$).

2.6. Geographical detector method to determine the drivers

The geographical detector method that was developed by Wang and Xu (2017) has been widely applied to detect the spatial stratified heterogeneity in the geographical variable Y (SOC) and to explore the influencing factors X behind it, with a hypothesis that the higher similarity of X and Y in the spatial distribution increases the importance of X (the influencing factors) (Qiao et al., 2019; Shi et al., 2018; Wang and Hu, 2012; Zhu et al., 2019b). The spatial stratified heterogeneity of

SOC can be quantified by Q-statistic values (q), and the factor detector module can be used to calculate the influence of these factors on the spatial distribution of SOC. The Q-statistic value was defined as follows:

$$q = 1 - \frac{\sum_{h=1}^{L} N_h \sigma_h^2}{N\sigma^2} \quad (7)$$

where q represents the Q-statistic value, L represents the number of strata, N represents the total number of field samples, N_h represents the number of samples in strata h, σ_h^2 is the variance of the geographical variable (SOC) in strata h, and σ^2 is the variance of the SOC in the whole study area. The geographical detector method was executed with the Geodetector software (Wang et al., 2016).

Based on previous studies (Liu et al., 2018a; Shi et al., 2014; Zhao et al., 2018), socioeconomic development is a significant contributor to SOC change, particularly for areas moving toward intensive urbanization. Thus, the changes in population density (Resource and Environment Data Cloud Platform, Chinese Academy of Sciences (RESDC, 2018e), GDP change (the change in Gross Domestic Product) (Resource and Environment Data Cloud Platform, Chinese Academy of Sciences (RESDC, 2018d), and density change in cropland areas representing the effects of economic growth (Resource and Environment Data Cloud Platform, Chinese Academy of Sciences (RESDC, 2018b), together with the changes in carbon inputs that were driven by economics and policy (Zhao et al., 2018), were chosen to quantify the degrees of influence on the temporal changes in SOC.

3. Results

3.1. Soil organic carbon contents

In 2011, the descriptive statistical results of the SOC contents in the areas of Shuyang, Rugao, and Shanghai are presented in Fig. 3. Overall, the median (min-max) of SOC contents in Shuyang, Rugao, and Shanghai were 13.60 (1.48–29.72) g kg^{-1}, 9.15 (3.59–16.25) g kg^{-1}, and 17.15 (5.65–32.63) g kg^{-1}, respectively. Coefficients of variation (CV) of the SOC content among the three study areas ranged from 29 % to 41%, at a moderate level (10–100% (Yu et al., 2019)). Compared to the mean SOC content in the topsoil (0–20 cm) that was estimated by Zhao et al. (2014a), the average SOC content in Rugao was slightly lower than that in Jiangsu Province (10.62 g kg^{-1}), while the mean SOC contents in Shuyang and Shanghai were relatively high.

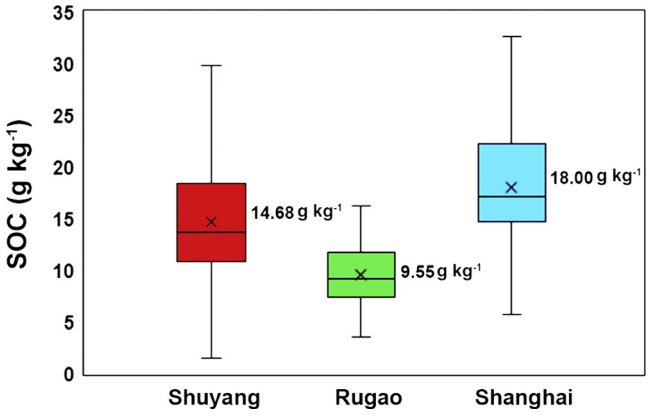

Fig. 3. Boxplots and descriptive statistics of the soil organic carbon contents in the Shuyang, Rugao, and Shanghai regions in 2011. (The cross points and solid lines in the boxes represent mean and median values; upper and lower edges and bars in or outside the boxes represent 75th and 25th, 95th and 5th percentiles of all data, respectively).

3.2. Spatial distribution of SOC and its drivers in topsoil

3.2.1. Spatial distribution of SOC

In Shuyang, the areas with high values of SOC were mainly distributed in the north (over 8 g kg^{-1} and 18 g kg^{-1} in 1981 and 2011, respectively), while the SOC contents in other parts of the study area were relatively low (e.g., < 6 g kg^{-1} in 1981 and < 14 g kg^{-1} in 2011 in the southern areas) (Fig. 4 **and Figure S3)**. However, there were local differences in the spatial distributions of SOC contents between the two dates. In 1981, the areas with high SOC contents (9.16 g kg^{-1}) were located in northwestern Shuyang (In the Typic Dark-Aquic Cambosols, **Table S3**). However, the areas with SOC lower than 10 g kg^{-1} in 2011 were very limited, where only located in the southwest (5.1 g kg^{-1}–10.0 g kg^{-1}). The SOC contents in most areas of Shuyang were more than 14 g kg^{-1}, particularly in the northeastern parts, where the SOC contents varied from 18.0 g kg^{-1} to 23.7 g kg^{-1} (e.g., in the Clay Loam Anthrostagnic Ochri-Aquic Cambosols, **Table S3**).

In Rugao city, the overall spatial distribution patterns of SOC contents were represented as high values of SOC in the southeast, and relatively low values of SOC in other parts, with ranges from 5.5 g kg^{-1} to 8.6 g kg^{-1} in 1981 and from 7.3 g kg^{-1} to 12.2 g kg^{-1} in 2011, respectively. In 1981, the SOC contents in most areas were less than 6 g kg^{-1}, excluding the southern parts of the study area (near the Yangtze River) where the SOC contents exceeded 8 g kg^{-1} (In the Loam Calcaric Ochri-Aquic Cambosols, **Table S3**). In 2011, the SOC contents ranged from 8 g kg^{-1} to 10 g kg^{-1} in most areas, except for SOC areas with SOC < 8 g kg^{-1} in the southwest of the study area (mainly in the Typic Fe-leachic Stagnic Anthrosols, **Table S3**).

In contrast, the spatial patterns of the SOC in Shanghai differed significantly between the two dates. In 1981, the areas with SOC > 20 g kg^{-1} were mainly located in the middle of the study area (21.8 g kg^{-1}–24.6 g kg^{-1}) (mainly in the Fe-accumulic Gleyi-Stagnic Anthrosols and the Endogleyic Fe-accumuli-Stagnic Anthrosols, **Table S3**), while the lowest-SOC areas showed a scattered distribution, with the SOC contents varying from 14.6 g kg^{-1} to 15.0 g kg^{-1}. However, in 2011, the SOC contents across the whole study area ranged from 15.0 g kg^{-1} to 22.4 g kg^{-1}, with a higher level of SOC content (> 20 g kg^{-1}) identified in the southwest (mainly in the Endogleyic Fe-accumuli-Stagnic Anthrosols, **Table S3**), and a low level of SOC content (< 18 g kg^{-1}) in the northeast (e.g., in the Typic Fe-accumuli-Stagnic Anthrosols, **Table S3**).

3.2.2. Drivers of spatial variability of SOC

Our results indicated that the terrain attributes (e.g., elevation), soil properties, vegetation (e.g., the NDVI), and human activities (e.g., crop carbon input) had different degrees of influence on the SOC in Shuyang, Rugao, and Shanghai. Therefore, these drivers were interpolated and divided into six classes with ArcGIS software (version of 10.2). Then, the geographical detector model was applied to quantify the importance of the predictors. As shown in Fig. 5, the variables of elevation (0.60) and Avk (0.57) played major roles in the spatial stratified heterogeneity of the SOC in Shuyang; the Sandy (0.70), BD (0.61), and elevation (0.51) could also predominantly explain the spatial variability of SOC in Rugao, while in Shanghai, the carbon inputs (0.68) and pH (0.65) were the main factors for the spatial distribution of SOC.

3.3. Temporal changes in SOC and the drivers in topsoil

3.3.1. Temporal changes in SOC and SOC storage

Significant differences in the SOC changes among the three county-level cities were observed, the SOC increased in Shuyang and Rugao, and significantly decreased in Shanghai over the period of 1981–2011 (Fig. 6). The areas in Shuyang with SOC increases greater than 6 g kg^{-1} were distributed throughout most of the study area, and a more significant increase in the SOC contents (increment > 10 g kg^{-1}) in the northeast were clearly observed (mainly in the Clay Loam

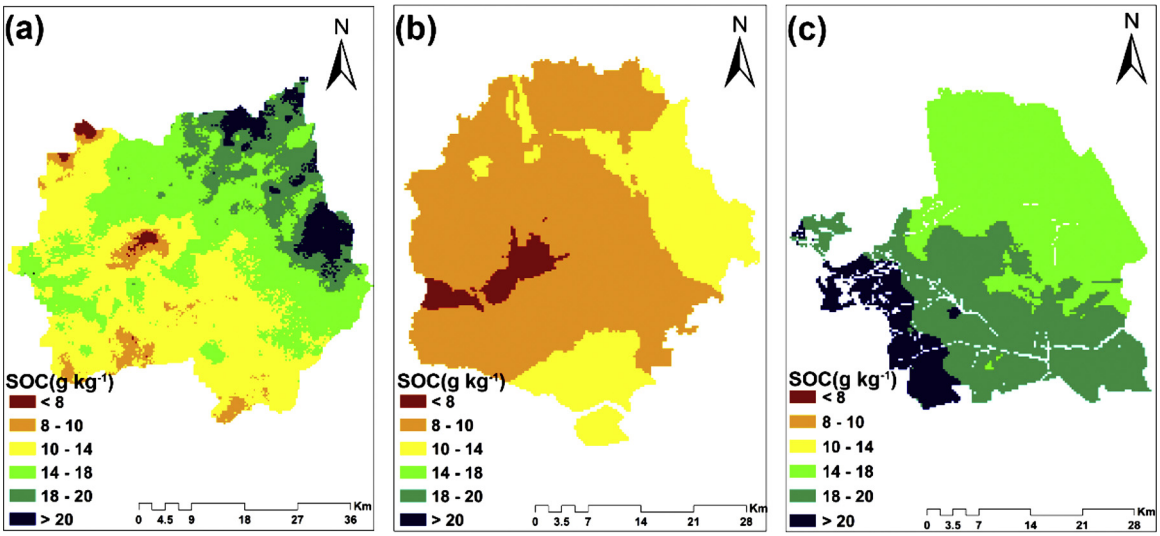

Fig. 4. Spatial distributions of the soil organic carbon (SOC) in Shuyang (a), Rugao (b), and Shanghai (c) regions in 2011.

Anthrostagnic Ochri-Aquic Cambosols and Loam Typic Hapli-Stagnic Anthrosols). Nevertheless, several areas with slight increases in SOC were also very limited and were mainly scattered in the northwest (green areas in Fig. 6), with increments less than 3 g kg^{-1}. In Rugao, an overall trend of relatively low increases in SOC (increments < 6 g kg^{-1}) occurred in the whole study area. The SOC contents in the southwest of the study area slightly increased, with a range of 0–3 g kg^{-1}, while the areas with larger SOC increments (3–6 g kg^{-1} were mainly identified throughout the whole study area (yellow areas) (e.g., in the Sandy Typic Hapli-Stagnic Anthrosols).

In Shanghai, the changes in the SOC contents across the study area varied from −9.23 g kg^{-1} to 5.46 g kg^{-1}. The spatial patterns of the changes in SOC over the past 30 years were characterized by strong decreases in the central and northern parts of the study area (e.g., in the Endogleyic Fe-accumuli-Stagnic Anthrosols), but slight increases in the southwest (e.g., in the Silt Loam Typic Hapli-Stagnic Anthrosols).

Over the last 30 years, the total soil carbon storage in topsoil increased from 3.99 Mt to 7.70 Mt in Shuyang and from 2.55 Mt to 3.74 Mt in Rugao, but decreased from 6.20 Mt to 4.85 Mt in Shanghai (Table 1). The mean SOCD in topsoil increased from 17.67 t ha^{-1} to 34.13 t ha^{-1} in Shuyang and from 16.63 t ha^{-1} to 24.34 t ha^{-1} in Rugao, but decreased from 52.93 t ha^{-1} to 41.44 t ha^{-1} in Shanghai **(Figure S4)**. Overall, the average SOC sequestration rates in Shuyang and Rugao over the past 30 years were +0.55 t ha^{-1} yr^{-1}, +0.26 t ha^{-1} yr^{-1}, respectively, which was significantly higher than that in Jiangsu Province (0.16 t ha^{-1} yr^{-1}) estimated by Liao et al. (2009) over the period of 1982−2004. While in Shanghai, although the average SOC sequestration rate was -0.38 t ha^{-1} yr^{-1}, the annual SOC loss (0.05 Mt yr^{-1}) was consistent with prior studies, such as the result (0.08 Mt yr^{-1}) estimated by Zhang et al. (2010).

3.3.2. Drivers of SOC temporal changes

In the study area, the geodetector model was used to quantified the effect intensities of the four drivers (the changes in population density, GDP change, density changes of cropland areas, and the change of carbon inputs) on the temporal changes of SOC. Compared to the changes in population density, GDP change, and the change of carbon inputs, the indicators of the change in the density of cropland areas in Shuyang (q = 0.16), Rugao (q = 0.09), and Shanghai (q = 0.24), had a higher degree of explanation for the changes in SOC (Fig. 7).

4. Discussion

4.1. Drivers of SOC spatial variability

In Shuyang, the elevation had a predominant influence on the spatial distribution of SOC, as it might just match the spatial distribution of the soil types (Barthold et al., 2013; Xin et al., 2013). The Clay Loam Anthrostagnic Ochri-Aquic Cambosols that were distributed in the plains area were mainly developed from the alluvial materials and lacustrine deposits, which usually have higher SOC contents (Huang et al., 2017). However, the Loam Anthrostagnic Ochri-Aquic Cambosols and the Sandy Calcaric Ochri-Aquic Cambosols located in the areas with higher elevations were mainly derived from the Yellow River alluvium,

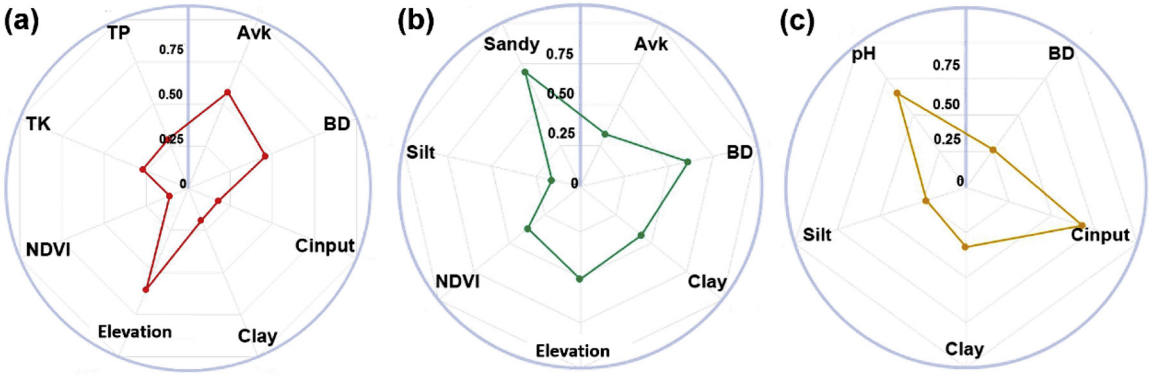

Fig. 5. Q-statistic values in the Geodetector analysis of the predictor importance for soil organic carbon (SOC) in Shuyang (a), Rugao (b), and Shanghai (c). (All variables in Fig. 5 showed strongly significant effects at $p < 0.05$).

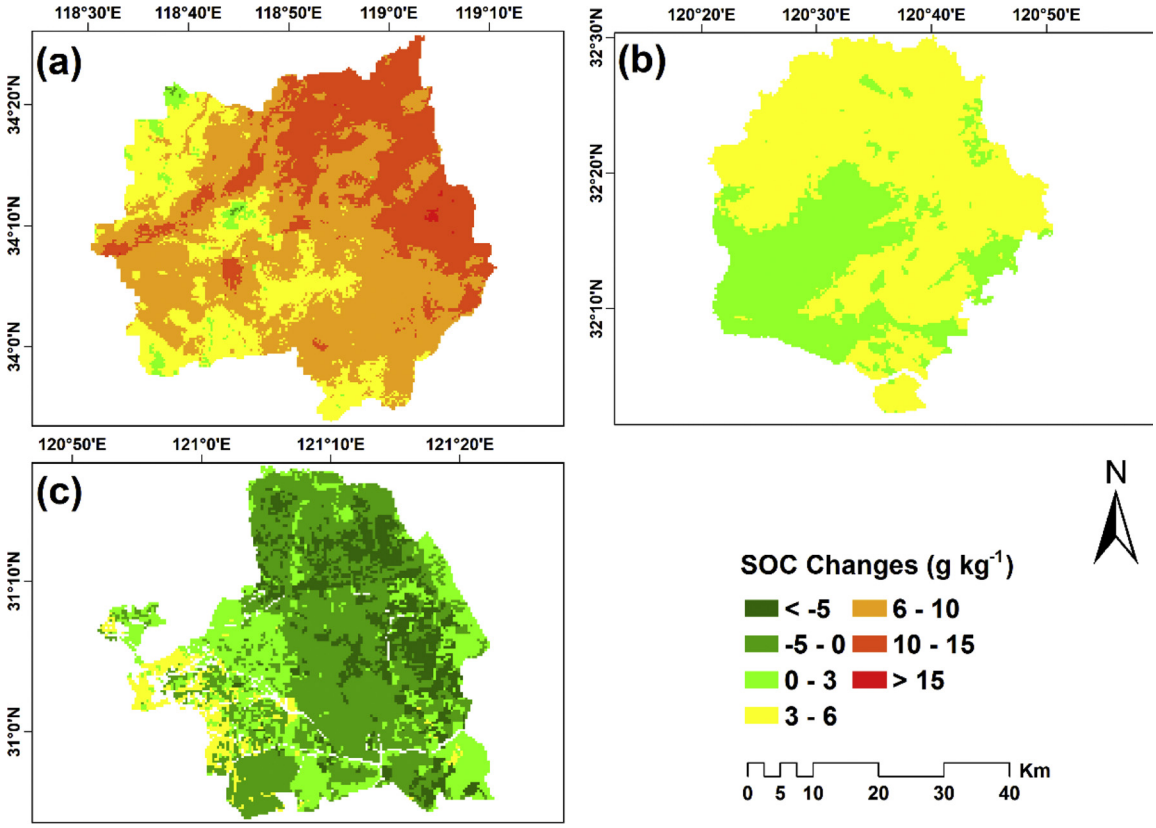

Fig. 6. Spatial patterns of the changes in soil organic carbon (SOC) during the period of 1981-2011 in Shuyang (a), Rugao (b), and Shanghai (c).

Table 1
Changes in SOC storage in the study area during 1981–2011.

County	C storage in 1981 (Mt)	C storage in 2011 (Mt)	C storage change (Mt)	Annual changes (t ha^{-1} yr^{-1})
Shuyang	3.99	7.70	3.71	0.55
Rugao	2.55	3.74	1.18	0.26
Shanghai	6.20	4.85	−1.35	−0.38

which is composed of sandy materials. The SOC contents in these soils were lower compared to other parts of Shuyang (Huang et al., 2017). Therefore, regional difference in the spatial distributions of the soil types resulting from the topographic feature were the main reason for the spatial variability of SOC in Shuyang.

Soil texture could significantly affect the spatial distribution of SOC as the clay and silt contents in soil texture mainly affect the formation of aggregate and protect SOC from decomposition, thus contributing SOC accumulation (Šimanský et al., 2019; Yost and Hartemink, 2019). However, in Rugao, soil such as the Sandy Typic Hapli-Stagnic Anthrosols, the Calcaric Typic Hapli-Stagnic Anthrosols, the Typic Haplic-Ustic Cambosols, and the Typic Fe-leachic Stagnic Anthrosols, which were widely distributed in western, central, and northeastern areas, were developed from alluvial materials (Fig. 1), causing relatively coarse textures among these soil series (Huang et al., 2007). Due to low silt and clay contents, the sandy soils (q = 0.70), which covered a large part of the study area, were identified as the most important factor affecting the spatial variation of SOC in Rugao, indicating the importance of silt and clay fractions in soil texture for the spatial distribution of SOC (Gonçalves et al., 2017).

Additionally, the factors of Avk and BD also played important roles in affecting the spatial variability of SOC in Shuyang and Rugao,

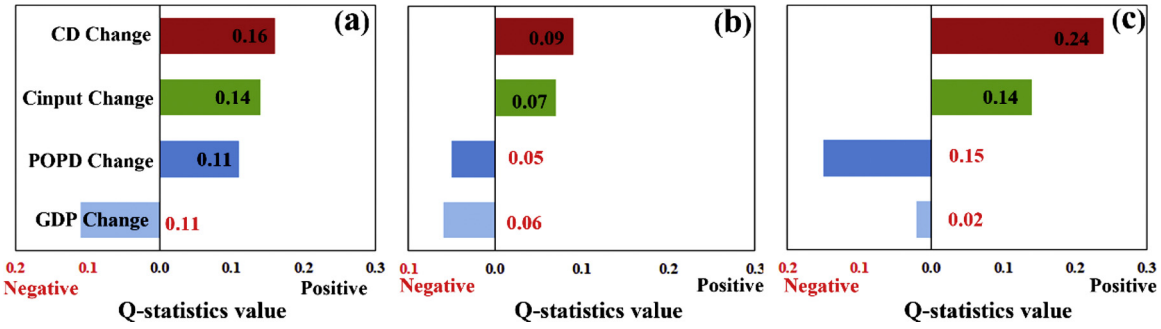

Fig. 7. The impact of human activities on the changes in soil organic carbon (SOC) in Shuyang (a), Rugao (b), and Shanghai (c). The population density changes from 1995 to 2015 (POPD change), the Gross Domestic Product changes from 1995 to 2015 (GDP change), and density changes in cropland areas from 1980 to 2010 (CD change) were obtained from RESDC (2018e), RESDC (2018d), and RESDC (2018b), respectively; the change of carbon input from 2000 to 2011 (Cinput change) was estimated using net primary production (NPP) data. The NPP data were obtained from the NTSG (2015).

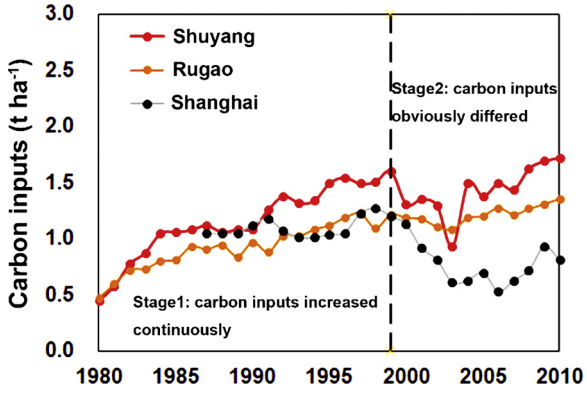

Fig. 8. Crop root carbon inputs since 1981 (carbon inputs by roots were estimated using the crop yield data referenced by Zhao et al. (2018)).

possibly due to the influence of intensive anthropogenic activities such as manure use (Nazeer and Malik, 2011), the use of chemical fertilizers (Blanchet et al., 2017; He et al., 2015), and tillage (Gwenzi et al., 2008; Nyamadzawo et al., 2007; Zhang et al., 2018). Farmers in the area rely on these agricultural management to improve crop yields, which results in the spatial variations of Avk and BD thus further affects the spatial change of SOC. Therefore, although the factors of elevation and soil types were the predominant drivers of the spatial distribution of SOC in Shuyang and Rugao, the impacts of the human activities (e.g., agricultural management practices) also have important contribution to spatial variations of SOC.

In contrast, the crop carbon input was identified as the most significant contributor to the spatial variability of SOC in Shanghai. SOC accumulation largely depended on the balance between the inputs such as the organic materials from aboveground and belowground parts of plants (Godbold et al., 2006), and the outputs from soil decomposition. The improvements from returning straw, above-ground residue, and roots to soil can significantly contribute to the increase in labile organic matter fractions through microbial decomposition and turnover, leading to accelerated accumulation of SOC (Li et al., 2018b). Thus, the quantity of straw return by different management practices may have been the main factor effecting SOC accumulation, which was consistent with the findings of previous studies (Sukhdev et al., 2011; Wang et al., 2015; Zheng et al., 2015).

In addition, as one of the most developed metropolis in China, Shanghai has experienced rapid urban expansion and industrialization over the last three decades (Gu et al., 2019). Topsoil pH value in Shanghai (6.57) was significantly lower than those in Shuyang (6.98) and Rugao (7.31). In the acidic soil, the pH values can certainly affect the process of SOC decomposition and turnover, including the decrease in SOC solubility (Vance and David, 1991), the composition of microbial species (Curtin et al., 1998; Motavalli et al., 1995; Shah et al., 1990), and the soil microbial/enzymatic activities (Haynes and Swift, 1988; Higashida and Takao, 1986; Van et al., 1998). Therefore, the contribution of soil pH to the predicted SOC was still very important due to intensive anthropogenic activities (i.e., the enhanced industrial emission and urban expansion).

4.2. Drivers of SOC temporal changes

Numerous studies have explored that land use change caused by human activities had a significant influence on changes in SOC (James et al., 2019; Jose et al., 2004; Meyer-Jacob et al., 2015; Wu et al., 2003). However in this study area, the local details of land use change differed significantly among the three county-level cities. In Shuyang, the area of paddy fields rapidly increased from 5×10^4 hectares (ha) in 1984 to 8×10^4 ha in 2010 (Xin et al., 2013). A significant increase in SOC was largely attributable to the change from dry land to paddy fields, where the microbial decay constrained the rate of SOC decomposition because of the anaerobic conditions during flooding seasons (Li et al., 2018a). Similarly, the land use was also changed from dry land to paddy fields in Rugao (Huang et al., 2007), thus resulting in slight increase in SOC during 1981–2011.

In Shanghai, the conversion from wetlands to cultivated lands (e.g., paddy field) resulted in SOC decrease during 1981–2011 (Ji, 2009). The types of planted vegetation were also changed from aquatic vegetation that requires special adaptations to live submerged in water (e.g., zizania, bulrush, water hyacinth) to agricultural crops, such as rice. The soil in the wetlands was saturated with water throughout the year, leading to a sufficiently anaerobic environment to constraint the rate of SOC decomposition compared with that in the paddy fields (Huang et al., 2010; Liu et al., 2017a; Liu et al., 2018b). Furthermore, with rapid urban expansion, a large area of cultivated lands have been further replaced by building lands (Cui and Shi, 2012). The land use changes resulting from rapid urbanization were a significant contributor to the accelerated loss of SOC in the surface soil because of the intensive human disturbance, which directly alters the stability of the soil aggregates by exposing surface SOC to microbial decomposition (Chen et al., 2014). Therefore, wetland reclamation and further degradation of the cultivated lands disturbed the balance of carbon inputs and outputs, leading to rapid decreases in SOC contents (Xu et al., 2019; Zhang et al., 2019b).

The plant-derived carbon input was another main anthropogenic factor affecting the SOC changes in Shuyang ($q = 0.14$), Rugao ($q = 0.07$), and Shanghai ($q = 0.14$) (Fig. 7). Across the field investigation in the study area, carbon inputs, which were calculated with the method from Zhao et al. (2018), from the period of 1981–2010 were shown in Fig. 8. The root-derived carbon inputs per hectare were characterized by minimal carbon inputs in 1981 and then continuous increases in Shuyang and Rugao, while in Shanghai, the carbon inputs have declined significantly since 2000. The net increments of carbon inputs by the roots in Shuyang (1981–2010), Rugao (1981–2010), and Shanghai (1987–2010) were 1.27 t ha^{-1}, 0.88 t ha^{-1}, and −0.24 t ha^{-1}, respectively, which was highly consistent with the temporal changes in SOC.

Moreover, the initial SOC contents also had a profound effect on the changes in SOC (Manns et al., 2007; Poirier et al., 2013). In the study area, the initial SOC contents in Shuyang (6.47 g kg^{-1}) and Rugao (6.26 g kg^{-1}) in 1981 were very low compared with those at the provincial level (9.60 g kg^{-1}) (Zhao et al., 2014a), but croplands in Shanghai had relatively high initial SOC contents (19.87 g kg^{-1}). The Steady increases in carbon inputs were the primary reasons leading to the SOC increases in Shuyang and Rugao due to the low initial SOC levels. However in Shanghai, with the implementation of the straw return practice, although the carbon inputs increased rapidly, low-level carbon inputs over a sufficiently long time period (1987–2007) could not maintain high-level SOC content. The plant-derived carbon inputs were quantitatively lower than carbon loss (e.g., soil microbial decomposition). Therefore, the insufficient organic carbon inputs (which imply excessive carbon loss), combined with the high-level initial SOC content, may be one of the major reasons for significant decreases in the SOC content in Shanghai (Zhao et al., 2018).

4.3. Implications and limitations

This paper confirms the differences on the spatiotemporal changes of SOC in three areas with different levels of economic development across the Jiangsu-Shanghai region. This work highlights that land use change is the most dominant contributor in affecting SOC temporal changes over the last three decades.

There are some limitations on the source of SOC data in 1981. As we mentioned in the section of materials and methods, GPS was not available in the early 1980s in China, and positions of all sampling sites were only recorded by text descriptions in 1981. However, the source of

SOC data in 1981 are from the second national soil survey of China which involved the most comprehensive and detailed historical soil database to date (Zhao et al., 2018).

Compared to the application of interpolation method in 2011, the ST method was used for mapping spatial distribution of SOC in 1981 when accurate position information was not considered. Uncertainties associated with different prediction methods may have occurred in the result. However, considering a lack of geographic coordinates for soil samples in 1981 and the reliability of SOC prediction in 2011, the subtraction from the ST-predicted SOC to the interpolation-predicted SOC has been considered as a reasonable method for calculating the SOC temporal changes. More importantly, these findings explored the spatiotemporal changes of SOC in a long run and drivers in typical economically developed areas in China, and to provide scientific support for agriculture policy making and environmental sustainable development in the areas experiencing similar socio-economic development.

5. Conclusion

Our results revealed that significant increases in SOC occurred in Shuyang and Rugao, and the SOC decreased in Shanghai over the period of 1981–2011. The spatial variability of SOC in this study was largely attributed to natural factors, including the elevation in Shuyang and the sand content in Rugao, while the variables of pH and carbon input, which were driven by human activities (e.g., straw return), were the main reasons for the spatial heterogeneity of SOC in Shanghai. The changes in land use types were identified as the largest drivers of the increases in SOC in Shuyang and Rugao (dryland farming to rice cultivation), and the decreases in SOC in Shanghai (wetland to rice cultivation). In addition, plant-derived carbon inputs were another major driver affecting the SOC changes in the cropland soils. Our results enriched our understanding of the regional differences in SOC changes and suggested that reasonable land use and effective management practices are essential for SOC accumulation, particularly in areas with rapid land use change.

Declaration of interests

The authors declare that they have no known competing financial interests or personal relationships that could have appeared to influence the work reported in this paper.

Declaration of Competing Interest

The authors report no declarations of interest.

Acknowledgments

The authors are grateful for the funding from the National Key Research and Development Program of China (2017YFA0603002) and the Strategic Priority Research Program of the Chinese Academy of Sciences (Grant No.XDA05050503).

Appendix A. Supplementary data

Supplementary material related to this article can be found, in the online version, at doi:https://doi.org/10.1016/j.still.2020.104763.

References

Barthold, F.K., Wiesmeier, M., Breuer, L., Frede, H.G., Wu, J., Blank, F.B., 2013. Land use and climate control the spatial distribution of soil types in the grasslands of Inner Mongolia. J. Arid Environ. 88, 194–205.
Blanchet, G., Libohova, Z., Joost, S., Rossier, N., Schneider, A., Jeangros, B., Sinaj, S., 2017. Spatial variability of potassium in agricultural soils of the canton of Fribourg, Switzerland. Geoderma 290, 107–121.
Brunsdon, C., Fotheringham, A.S., Charlton, M., 1996. Geographically weighted regression: a method for exploring spatial nonstationarity. Geogr. Anal. 28, 281–289.
Chen, Y., Day, S.D., Wick, A.F., McGuire, K.J., 2014. Influence of urban land development and subsequent soil rehabilitation on soil aggregates, carbon, and hydraulic conductivity. Sci. Total Environ. 494–495, 329–336.
Costa, E.M., Tassinari, W.S., Pinheiro, H.S.K., Beutler, S.J., Dos Anjos, L.H.C., 2018. Mapping soil organic carbon and organic matter fractions by geographically weighted regression. J. Environ. Qual. 47 (4), 718–725.
Cui, L., Shi, J., 2012. Urbanization and its environmental effects in Shanghai. China. Urban Climate 2, 1–15.
Curtin, D., Campbell, C.A., Jalil, A., 1998. Effects of acidity on minerali-zation: pH-dependence of organic matter mineralization in weakly acidic soils. Soil Biol. Biochem. 30, 57–64.
Fei, X., Christakos, G., Xiao, R., Ren, Z., Liu, Y., Lv, X., 2019. Improved heavy metal mapping and pollution source apportionment in Shanghai City soils using auxiliary information. Sci. Total Environ. 661, 168–177.
Fernandes, M.M.H., Coelho, A.P., Fernandes, C., Silva, M.F.D., Dela Marta, C.C., 2019. Estimation of soil organic matter content by modeling with artificial neural networks. Geoderma 350, 46–51.
Fissore, C., Dalzell, B.J., Berhe, A.A., Voegtle, M., Evans, M., Wu, A., 2017. Influence of topography on soil organic carbon dynamics in a Southern California grassland. Catena 149, 140–149.
Fotheringham, A.S., Brunsdon, C., Charlton, M., 2002. Geographically Weighted Regression: the Analysis of Spatially Varying Relationships. Wiley, England.
Frouz, J., 2018. Effects of soil macro- and mesofauna on litter decomposition and soil organic matter stabilization. Geoderma 332, 161–172.
Fujisaki, K., Chevallier, T., Chapuis-Lardy, L., Albrecht, A., Razafimbelo, T., Masse, D., Ndour, Y.B., Chotte, J.-L., 2018. Soil carbon stock changes in tropical croplands are mainly driven by carbon inputs: a synthesis. Agric. Ecosyst. Environ. 259, 147–158.
Gao, X., Xiao, Y., Deng, L., Li, Q., Wang, C., Li, B., Deng, O., Zeng, M., 2019. Spatial variability of soil total nitrogen, phosphorus and potassium in Renshou County of Sichuan Basin. China. J. Integr. Agr. 18 (2), 279–289.
Godbold, D.L., Hoosbeek, M.R., Lukac, M., Cotrufo, M.F., Janssens, I.A., Ceulemans, R., Polle, A., Velthorst, E.J., Scarascia-Mugnozza, G., De Angelis, P., Miglietta, F., Peressotti, A., 2006. Mycorrhizal hyphal turnover as a dominant process for carbon input into soil organic matter. Plant Soil 281 (1–2), 15–24.
Gonçalves, D.R.P., Sá, J.C.D.M., Mishra, U., Cerri, C.E.P., Ferreira, L.A., Furlan, F.J.F., 2017. Soil type and texture impacts on soil organic carbon storage in a sub-tropical agro-ecosystem. Geoderma 286, 88–97.
Gu, X., Xie, B., Zhang, Z., Guo, H., 2019. Rural multifunction in Shanghai suburbs: evaluation and spatial characteristics based on villages. Habitat Int. 92, 102041.
Guo, J.H., Liu, X.J., Zhang, Y., Shen, J.L., Han, W.X., Zhang, W.F., Christie, P., Goulding, K.W., Vitousek, P.M., Zhang, F.S., 2010. Significant acidification in major Chinese croplands. Science 327 (5968), 1008–1010.
Gwenzi, W., Gotosa, J., Chakanetsa, S., Mutema, Z., 2008. Effects of tillage systems on soil organic carbon dynamics, structural stability and crop yields in irrigated wheat (Triticum aestivum L.)–cotton (Gossypium hirsutum L.) rotation in semi-arid Zimbabwe. Nutr. Cycl. Agroecosys. 83 (3), 211–221.
Han, D., Wiesmeier, M., Conant, R.T., Kuhnel, A., Sun, Z., Kogel-Knabner, I., Hou, R., Cong, P., Liang, R., Ouyang, Z., 2018. Large soil organic carbon increase due to improved agronomic management in the North China Plain from 1980s to 2010s. Glob. Chang. Biol. 24 (3), 987–1000.
Hancock, G.R., Kunkel, V., Wells, T., Martinez, C., 2019. Soil organic carbon and soil erosion – understanding change at the large catchment scale. Geoderma 343, 60–71.
Haynes, R.J., Swift, R.S., 1988. Effects of lime and phosphate additions on changes in enzyme activities, microbial biomass and levels of extractable nitrogen, sulphur and phosphorus in an acid soil. Biol. Fert. Soils. 6, 153–158.
He, P., Yang, L., Xu, X., Zhao, S., Chen, F., Li, S., Tu, S., Jin, J., Johnston, A.M., 2015. Temporal and spatial variation of soil available potassium in China (1990–2012). Field Crop Res. 173, 49–56.
Higashida, S., Takao, K., 1986. Relations between soil microbial activity and some soil properties in grassland. Soil Sci. Plant Nutr. 32, 587–597.
Huang, B., Sun, W., Zhao, Y., Zhu, J., Yang, R., Zou, Z., Ding, F., Su, J., 2007. Temporal and spatial variability of soil organic matter and total nitrogen in an agricultural ecosystem as affected by farming practices. Geoderma 139 (3–4), 336–345.
Huang, Y., Sun, W., Zhang, W., Yu, Y., Su, Y., Song, C., 2010. Marshland conversion to cropland in northeast China from 1950 to 2000 reduced the greenhouse effect. Glob. Change Biol. 16 (2), 680–695.
Huang, B., Pan, J., Wang, P., Wang, H., Lei, X., Du, G., 2017. Soil Series of China, Jiangsu Volume. Science Press, Beijing.
Indorante, S.J., Hammer, R.D., Koenig, P.G., Follmer, L.R., 1990. Particle-Size analysis by a modified pipette procedure. Soil Sci. Soc. Am. J. 54, 560–563.
ISSCAS, 1978. Soil Physics and Chemistry Analysis. Shanghai Science & Technology Press, Shanghai.
James, J.N., Gross, C.D., Dwivedi, P., Myers, T., Santos, F., Bernardi, R., Faria, M.F.D., Guerrini, I.A., Harrison, R., Butman, D., 2019. Land use change alters the radiocarbon age and composition of soil and water-soluble organic matter in the Brazilian Cerrado. Geoderma 345, 38–50.
Jat, H.S., Datta, A., Choudhary, M., Yadav, A.K., Choudhary, V., Sharma, P.C., Gathala, M.K., Jat, M.L., McDonald, A., 2019. Effects of tillage, crop establishment and diversification on soil organic carbon, aggregation, aggregate associated carbon and productivity in cereal systems of semi-arid Northwest India. Soil Tillage Res. 190, 128–138.
Jensen, J.L., Schjønning, P., Watts, C.W., Christensen, B.T., Peltre, C., Munkholm, L.J., 2019. Relating soil C and organic matter fractions to soil structural stability.

Geoderma 337, 834–843.
Ji, Y., 2009. A Study on the Present Situation and Protection Countermeasure of Wetland Resources in Shanghai. East China Normal University, Shanghai.
Johannes, A., Matter, A., Schulin, R., Weisskopf, P., Baveye, P.C., Boivin, P., 2017. Optimal organic carbon values for soil structure quality of arable soils. Does clay content matter? Geoderma 302, 14–21.
Jose, M.G., Stephen, D.S., Dan, Y., F.Stuart, C.I., 2004. Impact of agricultural land-use change on carbon storage in Boreal Alaska. Glob. Change Biol. 10, 452–472.
Kang, D., Dall'erba, S., 2016. Exploring the spatially varying innovation capacity of the US counties in the framework of Griliches' knowledge production function: a mixed GWR approach. J. Geogr. Syst. 18 (2), 125–157.
Kononova, M.M., 1966. Soil Organic Matter. Its Nature, Its Role in Soil Formation and in Soil Fertility. Pergamon Press, New York.
Lehmann, J., Kleber, M., 2015. The contentious nature of soil organic matter. Nature 528 (7580), 60–68.
Li, Z., Li, D., Ma, L., Yu, Y., Zhao, B., Zhang, J., 2018. Effects of straw management and nitrogen application rate on soil organic matter fractions and microbial properties in North China Plain. J. Soil Sediment 19 (2), 618–628.
Li, H.Y., Wang, H., Wang, H.T., Xin, P.Y., Xu, X.H., Ma, Y., Liu, W.P., Teng, C.Y., Jiang, C.L., Lou, L.P., Arnold, W., Cralle, L., Zhu, Y.G., Chu, J.F., Gilbert, J.A., Zhang, Z.J., 2018a. The chemodiversity of paddy soil dissolved organic matter correlates with microbial community at continental scales. Microbiome 6 (1), 187.
Liao, Q., Zhang, X., Li, Z., Pan, G., Smith, P., Jin, Y., Wu, X., 2009. Increase in soil organic carbon stock over the last two decades in China's Jiangsu Province. Glob. Chang. Biol. 15 (4), 861–875.
Liu, W., Su, Y., Yang, R., Yang, Q., Fan, G., 2011. Temporal and spatial variability of soil organic matter and total nitrogen in a typical oasis cropland ecosystem in arid region of Northwest China. Environ. Earth Sci. 64 (8), 2247–2257.
Liu, X., Jiang, M., Dong, G., Zhang, Z., Wang, X., 2017a. Ecosystem service comparison before and after marshland conversion to paddy field in the Sanjiang Plain, Northeast China. Wetlands 37 (3), 593–600.
Liu, Y., He, N., Zhu, J., Xu, L., Yu, G., Niu, S., Sun, X., Wen, X., 2017b. Regional variation in the temperature sensitivity of soil organic matter decomposition in China's forests and grasslands. Glob. Chang. Biol. 23 (8), 3393–3402.
Liu, R., Wang, M., Chen, W., 2018a. The influence of urbanization on organic carbon sequestration and cycling in soils of Beijing. Landscape Urban Plan 169, 241–249.
Liu, X., Zhang, Y., Dong, G., Jiang, M., 2018b. Difference in carbon budget from marshlands to transformed paddy fields in the Sanjiang Plain, Northeast China. Ecol. Eng. 137, 60–64.
Lu, X., Shi, Y., Chen, C., Yu, M., 2017. Monitoring cropland transition and its impact on ecosystem services value in developed regions of China: a case study of Jiangsu Province. Land Use Policy 69, 25–40.
Magdoff, F., Weil, R., 2004. Soil Organic Matter in Sustainable Agriculture. CRC Press, Florida.
Manns, H.R., Maxwell, C.D., Emery, R.J.N., 2007. The effect of ground cover or initial organic carbon on soil fungi, aggregation, moisture and organic carbon in one season with oat (Avena sativa) plots. Soil Tillage Res. 96 (1-2), 83–94.
Meersmans, J., Van Wesemael, B., Goidts, E., Van Molle, M., De Baets, S., De Ridder, F., 2011. Spatial analysis of soil organic carbon evolution in Belgian croplands and grasslands, 1960-2006. Glob. Chang. Biol. 17 (1), 466–479.
Meyer-Jacob, C., Tolu, J., Bigler, C., Yang, H., Bindler, R., 2015. Early land use and centennial scale changes in lake-water organic carbon prior to contemporary monitoring. Proc. Natl. Acad. Sci. U. S. A. 112 (21), 6579–6584.
Motavalli, P.P., Palm, C.A., Parton, C.A., 1995. Soil pH and organic C dynamics in tropical forest soils: evidence from laboratory and simulation studies. Soil Biol. Biochem. 27, 1589–1599.
Nazeer, S., Malik, A.U., 2011. Effect of tillage systems and farm manure on various properties of soil and nutrient's concentration. Russian Agri. Sci. 37 (3), 232–238.
Numerical Terradynamic Simulation Group (NTSG), 2015. Annual Net Primary Production Dataset, During 2000-2011. http://files.ntsg.umt.edu/data/NTSG_Products/MOD17/.
Nyamadzawo, G., Chikowo, R., Nyamugafata, P., Nyamangara, J., Giller, K.E., 2007. Soil organic carbon dynamics of improved fallow-maize rotation systems under conventional and no-tillage in Central Zimbabwe. Nutr. Cycl. Agroecosys. 81 (1), 85–93.
Ogle, S.M., Breidt, F.J., Paustian, K., 2005. Agricultural management impacts on soil organic carbon storage under moist and dry climatic conditions of temperate and tropical regions. Biogeochemistry 72 (1), 87–121.
Ondrasek, G., Bakic Begic, H., Zovko, M., Filipovic, L., Merino-Gergichevich, C., Savic, R., Rengel, Z., 2019. Biogeochemistry of soil organic matter in agroecosystems & environmental implications. Sci. Total Environ. 658, 1559–1573.
Pan, G., Smith, P., Pan, W., 2009. The role of soil organic matter in maintaining the productivity and yield stability of cereals in China. Agric. Ecosyst. Environ. 129 (1–3), 344–348.
Poirier, V., Angers, D.A., Rochette, P., Whalen, J.K., 2013. Initial soil organic carbon concentration influences the short-term retention of crop-residue carbon in the fine fraction of a heavy clay soil. Biol. Fertil. Soils 49 (5), 527–535.
Qiao, P., Yang, S., Lei, M., Chen, T., Dong, N., 2019. Quantitative analysis of the factors influencing spatial distribution of soil heavy metals based on geographical detector. Sci. Total Environ. 664, 392–413.
Resource and Environment Data Cloud Platform, Chinese Academy of Sciences (RESDC), 2018a. DEM Data in Jiangsu Province. Resource and Environment Data Cloud Platform. http://www.resdc.cn/data.aspx?DATAID=284.
Resource and Environment Data Cloud Platform, Chinese Academy of Sciences (RESDC), 2018b. Land Use Type Dataset in China, During 1980-2010. Resource and Environment Data Cloud Platform. http://www.resdc.cn/data.aspx?DATAID=99.
Resource and Environment Data Cloud Platform, Chinese Academy of Sciences (RESDC), 2018c. The Net Primary Production (NPP) Data in China, During 2005-2011. Resource and Environment Data Cloud Platform. http://www.resdc.cn/data.aspx?DATAID=204.
Resource and Environment Data Cloud Platform, Chinese Academy of Sciences (RESDC), 2018d. Spatial Distribution of GDP Dataset in China, During 1995-2015. Resource and Environment Data Cloud Platform. http://www.resdc.cn/data.aspx?DATAID=252.
Resource and Environment Data Cloud Platform, Chinese Academy of Sciences (RESDC), 2018e. . Spatial Distribution of Population Dataset in China, During 1995-2015. Resource and Environment Data Cloud Platform. http://www.resdc.cn/data.aspx?DATAID=251.
Shah, Z., Adams, W., Haven, C.D.V., 1990. Composition and activity of the microbial population in an acidic upland soil and effects of li-ming. Soil Biol. Biochem. 22, 257–263.
Shanghai Bureau of Statistics, 2010. 2009 Shanghai Statistical Yearbook. China Statistics Press, Beijing.
Shen, Q., Wang, Y., Wang, X., Liu, X., Zhang, X., Zhang, S., 2019. Comparing interpolation methods to predict soil total phosphorus in the Mollisol area of Northeast China. Catena 174, 59–72.
Shi, X.Z., Yu, D.S., Warner, E.D., Pan, X.Z., Petersen, G.W., Gong, Z.G., Weindorf, D.C., 2004. Soil database of 1:1,000,000 digital soil survey and reference system of the chinese genetic soil classification system. Soil Horiz. 45 (4), 129.
Shi, S., Cao, Q., Yao, Y., Tang, H., Yang, P., Wu, W., Xu, H., Liu, J., Li, Z., 2014. Influence of climate and socio-economic factors on the spatio-temporal variability of soil organic matter: a case study of Central Heilongjiang Province. China. J. Integr. Agr 13 (7), 1486–1500.
Shi, T., Hu, Z., Shi, Z., Guo, L., Chen, Y., Li, Q., Wu, G., 2018. Geo-detection of factors controlling spatial patterns of heavy metals in urban topsoil using multi-source data. Sci. Total Environ. 643, 451–459.
Šimanský, V., Juriga, M., Jonczak, J., Uzarowicz, Ł., Stępień, W., 2019. How relationships between soil organic matter parameters and soil structure characteristics are affected by the long-term fertilization of a sandy soil. Geoderma 342, 75–84.
Singh, M., Sarkar, B., Bolan, N.S., Ok, Y.S., Churchman, G.J., 2019. Decomposition of soil organic matter as affected by clay types, pedogenic oxides and plant residue addition rates. J. Hazard. Mater. 374, 11–19.
Soil Survey Committee of Shuyang County, 1984. Soil Records in Shuyang County. Soil Survey Committee of Shuyang County, Jiangsu Province.
Soil Survey Office of Rugao County, 1987. Soil Records in Rugao County. Soil Survey Office of Rugao County, Jiangsu Province, Rugao.
Soil Survey Office of Shanghai City, 1988. Soil Records in Shanghai City. Soil Survey Office of Shanghai City, Shanghai.
Song, X., Yang, J., Zhao, M., Zhang, G., Liu, F., Wu, H., 2019. Heuristic cellular automaton model for simulating soil organic carbon under land use and climate change: a case study in eastern China. Agric. Ecosyst. Environ. 269, 156–166.
Sukhdev, S.M., Marvin, N., Elston, D.S., Brian, M., Miles, D., Dick, P., 2011. Long-term straw management and N ferrtilizer rate effects on quantity and quality of organic C and N and some chemical properties in two contrasting soils in western Canada. Biol. Fertil. Soils 47, 785–800.
Takata, Y., Funakawa, S., Akshalov, K., Ishida, N., Kosaki, T., 2007. Spatial prediction of soil organic matter in northern Kazakhstan based on topographic and vegetation information. Soil Sci. Plant Nutr. 53 (3), 289–299.
Tiessen, H., Cuevas, E., Chacon, P., 1994. The role of soil organic matter in sustaining soil fertility. Letters to Nature 371, 783–785.
Van, B.P.F., Nott, C.J., Bull, I.D., 1998. Organic geochemical studies of soils from the Rothamsted classical experiments- IV. Preliminary results from a study of the effect of soil pH on organic matter decay. Org. Geochem. 29, 1779–1795.
Vance, G.F., David, M.B., 1991. Forest soil response to acid and salt addition of sulfate: III. Solubilization and composition of dissloved organic carbon. Soil Sci. 151, 297–305.
Vasenev, V.I., Stoorvogel, J.J., Vasenev, I.I., Valentini, R., 2014. How to map soil organic carbon stocks in highly urbanized regions? Geoderma 226–227, 103–115.
Wang, J., Hu, Y., 2012. Environmental health risk detection with GeogDetector. Environ. Model. Softw. 33, 114–115.
Wang, J., Xu, C., 2017. Geodetector: principle and prospective (In Chinese). Acta Geographica Sinica 72 (1), 116–134.
Wang, J., Wang, X., Xu, M., Feng, G., Zhang, W., Lu, C.A., 2015. Crop yield and soil organic matter after long-term straw return to soil in China. Nutr. Cycl. Agroecosys. 102 (3), 371–381.
Wang, J., Zhang, T., Fu, B., 2016. A measure of spatial stratified heterogeneity. Ecol. Indic. 67, 250–256.
Wang, X., Li, Y., Gong, X., Niu, Y., Chen, Y., Shi, X., Li, W., 2019. Storage, pattern and driving factors of soil organic carbon in an ecologically fragile zone of northern China. Geoderma 343, 155–165.
Wang, D., Li, X., Zou, D., Wu, T., Xu, H., Hu, G., Li, R., Ding, Y., Zhao, L., Li, W., Wu, X., 2020. Modeling soil organic carbon spatial distribution for a complex terrain based on geographically weighted regression in the eastern Qinghai-Tibetan Plateau. Catena 187, 104399.
Wood, S.A., Tirfessa, D., Baudron, F., 2018. Soil organic matter underlies crop nutritional quality and productivity in smallholder agriculture. Agric. Ecosyst. Environ. 266, 100–108.
Wu, H., Guo, Z., Peng, C., 2003. Land use induced changes of organic carbon storage in soils of China. Glob. Chang. Biol. 9, 305–315.
Xin, Z., Huang, B., Dong, C., Weixia, S., Hu, W., Tian, K., 2013. Tempo-spatial variability of soil organic matter and total nitrogen in farmland and its affecting factors in Shuyang county, Jiangsu province (in Chinese). Soils 45 (3), 405–411.
Xu, X., 2018. Annual Normalized Difference Vegetation Index (NDVI) Datasets of China, During 2005-2011. Data Center for Resources and Environmental Sciences, Chinese

Academy of Sciences. http://www.resdc.cn.
Xu, S., Liu, X., Li, X., Tian, C., 2019. Soil organic carbon changes following wetland cultivation: a global meta-analysis. Geoderma 347, 49–58.
Yan, X., Cai, Z., Wang, S., Smith, P., 2011. Direct measurement of soil organic carbon content change in the croplands of China. Glob. Chang. Biol. 17 (3), 1487–1496.
Yang, J., 2017. Soil Series of China, Shanghai Volume. Science Press, Beijing.
Yang, S., Liu, F., Song, X., Lu, Y., Li, D., Zhao, Y., Zhang, G., 2019. Mapping topsoil electrical conductivity by a mixed geographically weighted regression kriging: a case study in the Heihe River Basin, northwest China. Ecol. Indic. 102, 252–264.
Yost, J.L., Hartemink, A.E., 2019. Soil Organic Carbon in Sandy Soils: A Review 158. pp. 217–310.
Yu, H., Zha, T., Zhang, X., Ma, L., 2019. Vertical distribution and influencing factors of soil organic carbon in the Loess Plateau. China. Sci. Total Environ. 693, 1–8.
Zeng, C., Yang, L., Zhu, A.X., Rossiter, D.G., Liu, J., Liu, J., Qin, C., Wang, D., 2016. Mapping soil organic matter concentration at different scales using a mixed geographically weighted regression method. Geoderma 281, 69–82.
Zhang, H., Shi, L., Shi, X., 2010. Notice of retraction: soil organic carbon storage of different land use types in Shanghai. The 2nd Conference on Environmental Science and Information Application Technology, Wuhan, Wuhan, pp. 689–692.
Zhang, C., Tang, Y., Xu, X., Kiely, G., 2011. Towards spatial geochemical modelling: use of geographically weighted regression for mapping soil organic carbon contents in Ireland. Appl. Geochem. 26 (7), 1239–1248.
Zhang, S., Lu, X., Zhang, Y., Nie, G., Li, Y., 2019a. Estimation of soil organic matter, total nitrogen and total carbon in sustainable coastal wetlands. Sustainability 11 (3), 667.
Zhang, Z., Wang, J.J., Lyu, X., Jiang, M., Bhadha, J., Wright, A., 2019b. Impacts of land use change on soil organic matter chemistry in the Everglades, Florida - a characterization with pyrolysis-gas chromatography–mass spectrometry. Geoderma 338, 393–400.
Zhang, Y., Wang, S., Wang, H., Ning, F., Zhang, Y., Dong, Z., Wen, P., Wang, R., Wang, X., Li, J., 2018. The effects of rotating conservation tillage with conventional tillage on soil properties and grain yields in winter wheat-spring maize rotations. Agr. Forest Meteorol. 263, 107–117.
Zhao, Y., Shi, X., Weindorf, D.C., Yu, D., Sun, W., Wang, H., 2006. Map scale effects on soil organic carbon stock estimation in North China. Soil Sci. Soc. Am. J. 70 (4), 1377–1386.
Zhao, Y., Xu, X., Darilek, J.L., Huang, B., Sun, W., Shi, X., 2008. Spatial variability assessment of soil nutrients in an intense agricultural area, a case study of Rugao County in Yangtze River Delta region. China. Environ. Geol. 57 (5), 1089–1102.
Zhao, M., Zhang, G., Wu, Y., Li, D., Zhao, Y., 2014a. Temporal and spatial variability of soil organic matter and its driving force in Jiangsu province, China (in Chinese). Acta Pedologica Sinica 51 (3), 448–458.
Zhao, Y., Xu, X., Hai, N., Huang, B., Zheng, H., Deng, W., 2014b. Uncertainty assessment for mapping changes in soil organic matter using sparse legacy soil data and dense new-measured data in a typical black soil region of China. Environ. Earth Sci. 73 (1), 197–207.
Zhao, Y., Wang, M., Hu, S., Zhang, X., Ouyang, Z., Zhang, G., Huang, B., Zhao, S., Wu, J., Xie, D., Zhu, B., Yu, D., Pan, X., Xu, S., Shi, X., 2018. Economics- and policy-driven organic carbon input enhancement dominates soil organic carbon accumulation in Chinese croplands. Proc. Natl. Acad. Sci. U. S. A. 115 (16), 4045–4050.
Zheng, L., Wu, W., Wei, Y., Hu, K., 2015. Effects of straw return and regional factors on spatio-temporal variability of soil organic matter in a high-yielding area of northern China. Soil Tillage Res. 145, 78–86.
Zheng, L., Xu, J., Tan, Z., Xu, L., Wang, X., 2019. Spatial Distribution of Soil Organic Matter Related to Microtopography and NDVI Changes in Poyang Lake, China. Wetlands. .
Zhou, R., Xianzhang, P., Changkun, W., Ya, L., Yanli, L., Rongjie, S., Xianli, X., 2013. Estimation method for inputs of organic matter to regional farmland-Taking Changwu county as a case study (in Chinese). Soils 45 (5), 862–867.
Zhu, M., Feng, Q., Qin, Y., Cao, J., Zhang, M., Liu, W., Deo, R.C., Zhang, C., Li, R., Li, B., 2019a. The role of topography in shaping the spatial patterns of soil organic carbon. Catena 176, 296–305.
Zhu, Z., Wang, J., Hu, M., Jia, L., 2019b. Geographical detection of groundwater pollution vulnerability and hazard in karst areas of Guangxi Province, China. Environ. Pollut. 245, 627–633.